DOI:10.13350/j.cjpb.230613

·论著·

丹参酮IIA对多房棘球蚴原头节体外活性及生长的影响*

彭妍[1],贾云超[1],卓怡呈[1],多小勇[1],张示杰[2**]
(1.石河子大学医学院,新疆石河子 832000;2.石河子大学医学院第一附属医院肝胆外科)

【摘要】 **目的** 探究丹参酮IIA对多房棘球蚴原头节体外活性及生长的影响。 **方法** 从沙鼠体内获取多房棘球蚴原头节并在体外培养3d后分别与250、500、1000 μmol/L丹参酮IIA共培养7 d,以DMEM为空白对照组,DMSO为溶剂对照组,显微镜下观察各组原头节形态及活性(活性良好的原头节不被伊红染色),计算存活率并绘制活力曲线;共培养24 h后用活性氧(ROS)测定试剂盒测定各组原头节的ROS水平;共培养2d后用Western blot检测各组原头节凋亡相关蛋白Bcl-2、Bax和Caspase-3相对表达量;扫描电镜观察共培养2 d时各组原头节表面显微结构。多房棘球蚴原头节与大鼠肝癌细胞共培养8~9周形成多房棘球蚴囊泡,囊泡分别与两对照组、250、500、1000 μmol/L丹参酮IIA共培养2 d,扫描电镜观察囊泡生发层显微结构。 **结果** 原头节与250、500、1000 μmol/L丹参酮IIA共培养2 d,随着药物浓度的升高原头节形态结构发生改变,虫体模糊不清且红染率升高,原头节活性受抑制;共培养2d时空白对照组、溶剂对照组活力分别为100%、(98.53±0.503)%,250、500和1000 μmol/L组多房棘球蚴原头节活力分别为(81.00±3.606)%、(63.97±3.275)%、(37.07±3.296)%($F=298.1$,$P<0.05$);第7 d时空白对照组和溶剂对照组多房棘球蚴原头节活力分别为(98.33±0.577)%、(93.90±0.529)%,250和500 μmol/L组多房棘球蚴原头节活力分别为(51.67±7.638)%、(9.37±6.075)%,均低于对照组($P<0.05$)。1000 μmol/L丹参酮IIA组杀伤作用最强,原头节均死亡。共培养24 h,各浓度丹参酮IIA组原头节ROS水平显著高于对照组(均$P<0.05$);共培养2 d,随药物浓度增加,各浓度丹参酮IIA组原头节Bcl-2表达减少,Bax和Caspase-3表达升高(均$P<0.05$)。扫描电镜观察各浓度丹参酮IIA组原头节显微结构出现不同程度破坏甚至破裂,空白对照组和溶剂对照组原头节结构正常;不同浓度丹参酮IIA与囊泡共培养2d后扫描电镜观察囊泡生发层显微结构,可见生发层细胞不同程度地出现脱落、破裂。空白对照组和溶剂对照组生发层细胞包膜完整、形态饱满,并可见大量小的生发囊。 **结论** 丹参酮IIA对多房棘球蚴原头节体外活性及生长具有抑制作用,该抑制作用可能与丹参酮IIA打破原头节抗氧化防御系统的平衡、诱导细胞凋亡及抑制生发层细胞生长有关。

【关键词】 多房棘球蚴;原头节;丹参酮IIA;凋亡
【中图分类号】 R383.33 【文献标识码】 A 【文章编号】 1673-5234(2023)06-0689-06

[*Journal of Pathogen Biology*. 2023 Jun;18(6):689-694.]

Effects of tanshinone IIA on the Activity and growth of *Echinococcus multilocularis* protoscoleces *in vitro*

PENG Yan[1], JIA Yunchao[1], ZUO Yicheng[1], DUO Xiaoyong[1], ZHANG Shijie[2] (1. *School of Medicine, Shihezi University, Shihezi* 832000, *Xinjiang, China*; 2. *Department of Hepatobiliary Surgery, the First Affiliated Hospital of Medical College of Shihezi University*)**

【Abstract】 **Objective** To investigate the effects of tanshinoneIIA on the activity and growth of *Echinococcus multilocularis* protoscoleces *in vitro*. **Methods** The protoscoleces were extracting from girbil and cultured in vitro for 3 days, and then co-cultured with 250, 500, 1000 mol/L tanshinone IIA for 7days, by using DMEM as a blank control group and DMSO as solvent control group. The morphology, activity of protoscoleces were observed through a microscope (The active protoscoleces did not stain by eosin), and the survival rate was calculated. The ROS were tested by a Reactive Oxygen Species (ROS) test kit after 24 hours. Test the expression of apoptosisrelated proteins Bcl-2, Bax and Caspase-3 protein in each group by western blotting after 2 days. Scanning electron microscope was used to observe the surface microstructure of protoscoleces after 2 days. The protoscoleces were co-cultured with rat hepatoma cells for 8-9 weeks to form E. multilocularis vesicles, The vesicles were co-cultured with blank control group, solvent control group, and 250, 500, 1000 mol/L tanshinone IIA groups for 2 days, and the micros-tructure of The germinal layer of vesicles was observed by scanning electron microscope. **Results** Tanshinone IIA at concentrations of 250, 500, and 1000 mol/L changed the morphology and structure of protoscoleces, blurred the larvae and increased the red staining rate, and inhibited the activity

* 【基金项目】 国家自然科学基金项目(No. 8176120052)。
** 【通讯作者】 张示杰,E-mail:zhangshijie1@sina.com
【作者简介】 彭 妍(1994-)女,陕西宝鸡人,肿瘤学硕士。研究方向:肝胆良、恶性肿瘤研究。E-mail:1143089267@qq.com

of protoscoleces. After co-cultured for 2 days, the viability ofprotoscoleces inthe blank control group was 100% and the viability ofprotoscoleces in the solvent control group was (98.53±0.503)%, the viability ofprotoscoleces in 250, 500 and 1000 μmol /L groups were (81.00±3.606)%, (63.97±3.275)% and (37.07±3.296)% ($F=298.1$, $P<0.05$). On day 7, the viability ofprotoscoleces in blank control group and solvent control groupwere (98.33±0.577)% and (93.90±0.529)% , and than in the 250 and 500 μmol /L groups were (51.67±7.638)%, (9.37±6.075)% , respectively, which were significantly lower than those in the control group ($P<0.05$). The 1000 μmol/L tanshinone IIA group had the strongest killing effect, and all protoscoleces died. After co-cultured for 24 hours, the ROS was significantly higher in protoscoleces than control group. After co-cultured for 2 days, Bcl-2 expression decreased as the concentration of the drug increase, while Bax and Caspase-3 increased ($P<0.05$ for all). Scanning electron microscope showed that the microstructure of prot-oscoleces were damaged to varying degrees or even ruptured, while the structure of protoscoleces were normal in the blank control group and the solvent control group. After 2 days of co-culture with different concentrations of tanshinone IIA, the microstructure of the germinal layer cells of vesicles were observed by scanning electron microscope show that the germinal layer cells were exfoliated and ruptured to varying degrees. The germinal layer cells in the blank and the solvent control group had complete envelope, full shape, and a large number of small germinal vesicles. **Conclusion** Tanshinone IIA inhibited the activity and growth of the *E. multilocularis* protoscoleces in vitro, this inhibitory effect may be related to tanshinone IIA breaking the balance of the antioxidant defense system of protoscoleces, inducing cell apoptosis and inhibiting the growth of germinal layer cells.

【Key words】 *Echinococcus multilocularis*; protoscoleces; tanshinone IIA; apoptosis

多房棘球蚴病(alveolar echinococcosis, AE)是一种人兽共患寄生虫病,全球每年报道的新感染病例中大多数在中国[1]。AE隐匿起病,初次感染常在10年及以上才会有明显症状[2]。目前AE首选外科手术治疗,但大多数患者就诊时已有较广泛的肝脏浸润及转移而无法实施手术,需要药物治疗[3]。常用的抗AE药物为苯丙咪唑类药物,包括阿苯达唑等[4],但长期服用此类药物会引发相关不良反应[5],且存在药物的肠道吸收率低、起效时间长等问题,严重阻碍AE的治愈,因此亟待研发高效且不良反应小的抗AE药物。

中草药已经成为一种安全、无毒且易得的癌症治疗药物来源[6],从植物中提取的某些物质可诱导癌细胞凋亡[7]。丹参酮IIA(TanshinoneIIA, TanIIA)为植物丹参提取物[8-9],在传统中医中被广泛采用并用于治疗心血管疾病[10-12]。有充分证据表明,丹参酮IIA具有抗炎活性[13-14]和抗氧化性能[15-16]。大量研究显示,丹参酮IIA具有抗肿瘤作用,其机制主要有抑制肿瘤细胞增殖、诱导肿瘤细胞凋亡[17]等。本研究拟在体外用丹参酮IIA与多房棘球蚴原头节共培养,观察药物浓度对多房棘球蚴原头节活性及生长的影响,以期为AE晚期患者的保守治疗,手术后预防复发及药物的辅助治疗提供新思路。

材料与方法

1 材料

1.1 *动物、细胞及多房棘球蚴原头节* 长爪沙鼠购于新疆维吾尔自治区疾控中心。多房棘球蚴原头节取自本室腹腔保种的长爪沙鼠。大鼠肝癌细胞(H4-II-E-C3)购于上海富衡生物科技有限公司。

1.2 *主要试剂与仪器* 丹参酮IIA(TanshinoneIIA, TanIIA)、活性氧测定试剂盒和DMSO购自Solarbio(北京)公司;DMEM购自美国Life-Gibco公司;Bcl-2(ab196495)和Caspase-3(ab184787)购自美国abcam公司;Bax(#2772)和GAPDH(#5174)购自美国CST公司。SU8010扫描电镜为日本日立公司生产。

2 方法

2.1 *多房棘球蚴原头节的采集及体外培养* 参考卓怡呈等[18]的方法提取并提纯多房棘球蚴原头节,用完全培养基培养3 d用于后续试验。

2.2 *丹参酮IIA溶液配置* 丹参酮IIA溶液需现用现配。用DMSO溶解丹参酮IIA粉末,超声粉碎仪研磨混匀,用完全培养基将其配成目标浓度,DMSO终浓度不超过0.1%。

2.3 *丹参酮IIA与多房棘球蚴原头节共培养试验* 试验分为空白对照组、溶剂对照组(DMSO浓度不超过0.1%)和丹参酮IIA250、500、1000 μmol/L组,用六孔板进行培养,每孔加5 ml培养液和5 000个原头节,细胞培养箱中培养7 d,显微镜观察原头节的形态、伊红染色情况并计算红染率,绘制活力曲线图。原头节红染率(%)=(被染红的原头节数/原头节总数)×100%。原头节活性率(%)=1−原头节红染率(%)。

2.4 *原头节ROS检测* 对照组及各浓度丹参酮IIA组培养24 h后用PBS洗板3次,吸除PBS;荧光探针根据活性氧试剂盒说明书稀释后加入每组原头节中,于37 ℃恒温箱中孵育30 min,PBS洗3次,荧光显微镜观察各组原头节ROS水平。

2.5 *Bax、Bcl-2、Caspase-3测定* 采用Western blot

法。丹参酮IIA作用48 h后用PBS清洗各组原头节3次，提取原头节总蛋白，经SDS-PAGE电泳后湿转膜，TBST（含5%脱脂奶粉）常温封膜2 h，洗涤；加入相应一抗（兔抗鼠GAPDH、Bax、Bcl-2均为1∶1000稀释，兔抗鼠Caspase-3 1∶2000稀释），4 ℃摇床上孵育16 h，洗膜（TBST溶液）3次，每次5 min；加入二抗（1∶20000稀释的山羊抗兔IgG），摇床孵育1 h，PBS洗膜3次；滴加适量显影液（等量A、B液混匀），放入显影仪显影，测定相应蛋白的表达，Image-J软件处理条带，根据灰度值计算蛋白的相对表达量。

2.6 *扫描电镜观察原头节表面及囊泡生发层显微结构* 与丹参酮IIA共培养48 h后的原头节和与丹参酮IIA共培养48 h后的囊泡（原头节与大鼠肝癌细胞共培养8～9周后长成囊泡）用PBS清洗3次，每次5 min；将原头节和囊泡分别置于EP管中，用5%戊二醛固定液4 ℃固定24 h，pH7.2、0.1 mol/L PBS室温冲洗浸泡3次，每次20 min，吸弃磷酸缓冲液；于4 ℃用递增浓度的乙醇脱水，每次20 min；标本置临界点干燥仪充分干燥，固定于样品台上喷金，扫描电镜下观察原头节及囊泡的显微结构。

2.7 *统计学分析* 所有试验均重复3次及以上，采用GraphPad Prism 9.4.0软件进行统计学分析，结果以平均值±标准偏差（$\bar{x}\pm s$）表示。多组间比较采用重复测量方差分析和单因素方差分析（ANOVA）；多个实验组与对照组间比较采用Dunnett法。$P<0.05$为差异有统计学意义。

结 果

1 丹参酮IIA对体外培养的多房棘球蚴原头节内ROS的影响

250、500、1000 μmol/L丹参酮IIA与原头节共培养24 h，使用ROS测定试剂盒对原头节进行染色，荧光显微镜可见各组原头节均有荧光表达（图1），其中实验组荧光较强，且荧光强度与丹参酮IIA浓度成正比。对照组荧光强度较弱。

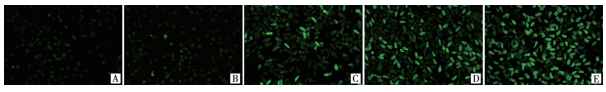

A 空白对照组 B 溶剂对照组 C 250 μmol/L丹参酮IIA组 D 500 μmol/L丹参酮IIA组 E 1000 μmol/L丹参酮IIA组

图1 荧光探针检测不同浓度丹参酮IIA体外作用24h的多房棘球蚴原头节ROS水平（50×）

A Blank control group B Solvent control group(DMSO) C 250 μmol/LtanshinoneIIA D 500μmol/LtanshinoneIIA E 1000 μmol/LtanshinoneIIA

Fig. 1 ROS levels in different concentrations of protoscoleces of *E. multilocularis* treated with tanshinone IIA for 24 hours *in vitro* (50×)

2 丹参酮IIA对体外培养的多房棘球蚴原头节形态的影响

空白对照组和溶剂对照组培养2 d，原头节多为顶突凹陷呈圆形或椭圆形，小钩排列整齐，虫体边缘清晰锐利，可见虫体内钙颗粒（图2A、2B）。不同浓度丹参酮IIA与原头节共培养2 d，250 μmol/L组原头节部分呈外翻型，虫体边缘尚清晰，原头节红染数量增加（图2C）；500 μmol/L组原头节外翻型比例增加，虫体边缘开始变模糊（图2D）；1000 μmol/L组原头节全为外翻型，小钩排列紊乱，虫体模糊不清，伊红染色可见红染数量明显增加（图2E）。

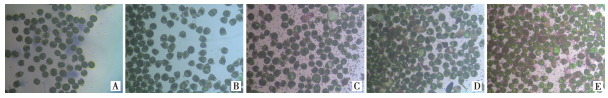

A 空白对照组 B 溶剂对照组 C 250 μmol/L丹参酮IIA组 D 500 μmol/L丹参酮IIA组 E 1000 μmol/L丹参酮IIA组

图2 不同浓度丹参酮IIA体外作用2 d的多房棘球蚴原头节形态（伊红染色，100×）

A Blank control group B Solvent control group(DMSO) C 250 μmol/LtanshinoneIIA D 500 μmol/LtanshinoneIIA E 1000 μmol/LtanshinoneIIA

Fig. 2 Morphological of protoscoleces of different concentrations of *E. multilocularis* treated with tanshinone IIA for 2 days *in vitro* (Eosin staining, 100×)

3 丹参酮IIA对体外培养的多房棘球蚴原头节活性的影响

不同浓度丹参酮IIA处理多房棘球蚴原头节7 d后，用0.1%伊红染色，观察原头节红染情况，计算原头节的存活率并绘制活力曲线（图3）。试验第2 d空白对照组、溶剂对照组活力分别为100%、（98.53±0.503）%，250、500和1000 μmol/L组多房棘球蚴原头节活力分别为（81.00±3.606）%、（63.97±3.275）%、（37.07±3.296）%（$F=298.1$，$P<0.05$）。第7 d时空白对照组和溶剂对照组多房棘球蚴原头节活力分别为（98.33±0.577）%、（93.90±0.529）%，250和500 μmol/L组多房棘球蚴原头节活力分别为（51.67±7.638）%、（9.37±6.075）%，1000 μmol/L组原头节均死亡（$F=330.5$，$P<0.05$）。表明提高丹参酮IIA的浓度及延长药物作用时间其对原头节活性的抑制作用增强。

4 丹参酮IIA对体外培养的多房棘球蚴原头节相关凋亡蛋白表达的影响

不同浓度丹参酮IIA（250、500、1000 μmol/L）与原头节共培养2 d后采用Western blot检测凋亡相关蛋白表达情况，结果如图4。随丹参酮IIA浓度增加，Bcl-2相对表达量逐渐降低且均低于空白对照组（$F=11.15$，$P<0.05$），Bax、caspase-3相对表达量逐渐增高且均高于空白对照组（$F=11.23$、6.375，$P<0.05$）。空白对照组与溶剂对照组比较3种蛋白的相

对表达量差异无统计学意义($P>0.05$)。

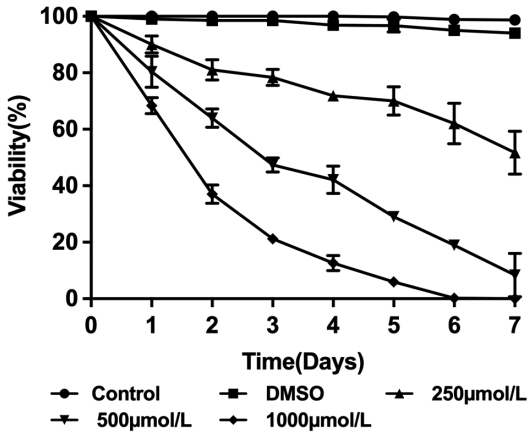

图 3 不同浓度丹参酮 IIA 体外作用后的多房棘球蚴原头节活力曲线
Fig. 3 Vitality curve of different concentrations of tanshinone IIA treated with *E. multilocularis* protoscoleces in vitro

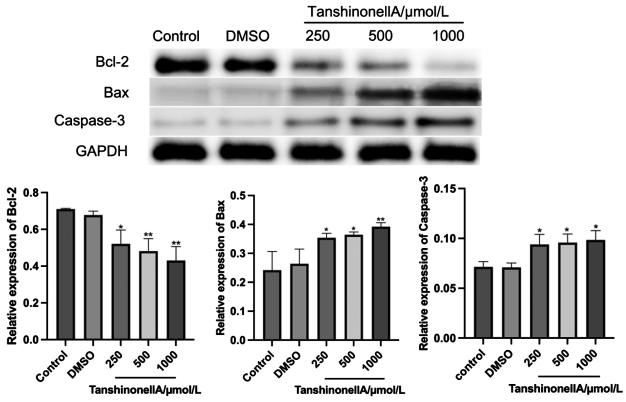

图 4 多房棘球蚴原头节与不同浓度丹参酮 IIA 共培养 2 d Bcl-2、Bax、Caspase-3 蛋白表达情况
Fig. 4 Expression of Bcl-2, Bax, and Caspase-3 proteins in 2days co-culture of different concentrations of tanshinone IIA with *E. multilocularis* protoscoleces

5 丹参酮 IIA 对多房棘球蚴原头节表面显微结构的影响

扫描电镜观察培养 2 d 的空白对照组和溶剂组原头节表面光整，顶突及顶突小钩结构正常、清晰，吸盘对称分布且中央凹陷，微绒毛排列整齐(图 5A、5B)。原头节与不同浓度丹参酮 IIA 共培养 2 d 后扫描电镜观察，250 μmol/L 组虫体顶突结构开始瓦解，虫体粗糙，微绒毛紊乱(图 5C)；500 μmol/L 组虫体出现破裂，顶突吸盘等结构消失，微绒毛消失(图 5D)；1000 μmol/L 组虫体部分结构消失，失去正常形态(图 5E)。

6 丹参酮 IIA 对多房棘球蚴囊泡生发层显微结构的影响

多房棘球蚴原头节与大鼠肝癌细胞共培养 8～9 周长成多房棘球蚴囊泡。扫描电镜观察培养 2 d 的空白对照组和溶剂组多房棘球蚴囊泡生发层细胞包膜完整、光滑圆润，可见大量小的生发囊(图 6A、图 6B)。囊泡与不同浓度丹参酮 IIA 共培养 2 d，250 μmol/L 组生发层细胞出现脱落，但仍可见少量小的生发囊存在(图 6C)；500 μmol/L 组部分生发层细胞出现脱落、破裂，未见小的生发囊存在(图 6D)；1000 μmol/L 组生发层细胞全部破裂(图 6E)。

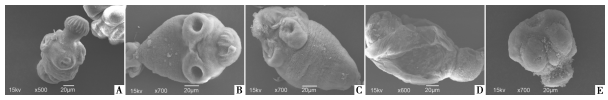

A 空白对照组 B 溶剂对照组 C 250 μmol/L 丹参酮 IIA D 500 μmol/L 丹参酮 IIA E 1000 μmol/L 丹参酮 IIA 组

图 5 扫描电镜下观察不同浓度丹参酮 IIA 作用 2d 后多房棘球蚴原头节表面微结构

A Blank control group B Solvent control group C 250 μmol/LtanshinoneIIA D 500 μmol/LtanshinoneIIA E 1000 μmol/LtanshinoneIIA

Fig. 5 Scanning electron microscopy was used to observe the surface microstructure of *E. multilocularis* protoscoleces after treatment with different concentrations of tanshinone IIA for 2 day

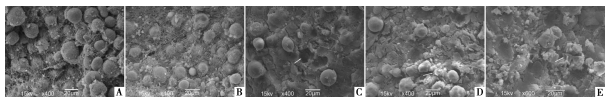

A 空白对照组 B 溶剂对照组 C 250 μmol/L 丹参酮 IIA 组 D 500 μmol/L 丹参酮 IIA 组 E 1000 μmol/L 丹参酮 IIA 组

图 6 扫描电镜观察不同浓度丹参酮 IIA 作用 2 d 后的多房棘球蚴囊泡生发层显微结构

A Blank control group B Solvent control group C 250 μmol/LtanshinoneIIA D 500 μmol/LtanshinoneIIA E 1000 μmol/LtanshinoneIIA

Fig. 6 Scanning electron microscopy was used to observe the sMicroscopic structure of the germinal layer of *E. multilocularis* vesicles after treatment with different concentrations of tanshinone IIA for 2 days

讨 论

目前关于抗肿瘤药物用于治疗 AE 的研究倍受关注。Hemer 等[19]报道伊马替尼可杀灭多房棘球蚴原头节、囊泡及生发层细胞。丹参酮ⅡA 最初被用来治疗心血管疾病，最近的研究表明该药有抗肿瘤作用，可阻碍肿瘤细胞的增殖、促使肿瘤细胞发生凋亡、引起肿瘤细胞分化、逆转肿瘤的耐药性等[20-21]。丹参酮ⅡA 与其他药物联合应用可提高化疗敏感性和疗效[22]。Jung 等[23]报道丹参酮ⅡA 可与隐丹参酮协同促进人白血病 K562 细胞凋亡。本研究结果显示，多房棘球蚴原头节与丹参酮 IIA 共培养，其红染率随药物浓度的增高及作用时间的延长呈上升趋势，活性呈下降趋势。扫描电镜观察显示药物对原头节结构具有破坏作用，而对照组原头节红染率及显微结构变化不明显，因此排除了所用溶剂剂量对原头节活性的影响，表明丹参酮 IIA 对原头节活性有抑制作用，与谭小武等[24]报道的黄腐酚在体外可抑制原头节活性甚至杀死原头节，且呈浓度和时间依赖的结果相似。

多房棘球蚴原头节活性的降低可能与丹参酮 IIA

诱导细胞凋亡有关。经典的线粒体和死亡受体凋亡途径均会引起 Caspase-3 的活化而使细胞发生凋亡[25]。Bcl-2 家族中的抗凋亡蛋白 Bcl-2、Bcl-w、Bcl-xL 等和促凋亡蛋白 Bax 和 Bak 等[26]在细胞凋亡中起关键作用[27]。有研究发现在正常情况下 Bcl-2/Bax 处于动态平衡，Bcl-2/Bax 值高于动态平衡可促使细胞存活，反之促使细胞发生凋亡[28]。本研究中丹参酮 IIA 作用后的多房棘球蚴原头节 Bcl-2 蛋白表达被抑制，而 Bax 和 Caspase-3 蛋白表达增加，且随药物浓度的提高该抑制及增加作用更明显。Li 等[29]报道丹参酮 IIA 浓度高时可促使发生 Caspase 蛋白依赖性的细胞凋亡，其机制与 Bax/Bcl-2 比值的增高、EGFR 和 LC3-2 降低、激活 Caspase-8 和 Caspase-3 等有关。以上表明丹参酮 IIA 可能同时通过内源性和外源性细胞凋亡途径抑制多房棘球蚴原头的节活性及生长，并促使其凋亡。

氧化应激同样对细胞凋亡起重要作用[24]，当 ROS 增多时可激活细胞凋亡[30]。内源或者外源性的细胞毒性物质及小分子等同样会引起 ROS 的提高，丹参酮 IIA 作为小分子化合物可能通过提高细胞内 ROS 水平使细胞发生凋亡[31]。本研究中随着丹参酮 IIA 浓度的增加 ROS 水平增高，表明丹参酮 IIA 可通过上调 ROS 介导多房棘球蚴原头节凋亡，与 Chiu 等[32]报道的丹参酮 IIA 可通过增加 ROS 的诱导导致非小细胞肺癌 A549 细胞凋亡结果相一致。

多房棘球蚴的生发层中存在生发细胞，是唯一可以增殖的细胞类型，可进行自我更新[33]，多房棘球蚴中所有分化的细胞都来源于生发细胞[34]。生发细胞是多房棘球蚴泡囊和原头节生长发育的重要基础[35]。本研究中随着丹参酮 IIA 浓度的增加，扫描电镜观察到囊泡生发层网状纤维保护作用逐渐减弱、生发层细胞数量减少、脱落、破裂，生发小囊数量减少或消失，这将导致多房棘球蚴的增殖受抑制，与 Cheng 等[36]报道的在生发层细胞的生长过程中使用酪氨酸激酶抑制剂后生发层细胞增值减弱、凋亡增加的结果相近。Xue 等[37]的研究同样发现丹参酮 IIA 以剂量依赖的方式抑制结肠癌 SW620 细胞增值。

本研究初步观察了不同浓度丹参酮 IIA 对多房棘球蚴原头节活性及生长的影响，结果显示丹参酮 IIA 对其活性及生长具有抑制作用，可能与丹参酮 IIA 激活原头节细胞凋亡信号通路有关，其具体机制有待进一步探讨。

【参考文献】

[1] Wen H, Vuitton L, Tuxun T, et al. Echinococcosis: advances in the 21st century[J]. Clin Microbiol Rev, 2019, 32(2): e00075-18.

[2] McManus DP, Zhang W, Li J, et al. Echinococcosis[J]. Lancet, 2003, 362(9392): 1295-1304.

[3] Hemphill A, Stadelmann B, Rufener R, et al. Treatment of echinococcosis: albendazole and mebendazole what else? [J]. Parasite, 2014, 21: 70.

[4] Hemphill A, Spicher M, Stadelmann B, et al. Innovative chemotherapeutical treatment options for alveolar and cystic echinococcosis[J]. Parasitology, 2007, 134(12): 1657-1670.

[5] Reuter S, Jensen B, Buttenschoen K, et al. Benzimidazoles in the treatment of alveolar echinococcosis: a comparative study and review of the literature[J]. JAntimicrob Chemother, 2000, 46(3): 451-456.

[6] Shaikh AS, Thomas AB, Chitlange SS. Herbdrug interaction studies of herbs used in treatment of cardiovascular disorders-A narrative review of preclinical and clinical studies[J]. Phytother Res, 2020, 34(5): 1008-1026.

[7] Cosson P, Hastoy C, Errazzu LE, et al. Genetic diversity and population structure of the sweet leaf herb, Stevia rebaudiana B., cultivated and landraces germplasm assessed by EST-SSRs genotyping and steviol glycosides phenotyping[J]. BMC Plant Biol, 2019, 19(1): 1-11.

[8] Chen AJ, Zhang JY, Li CH, et al. Separation and determination of active components in Radix Salviae miltiorrhizae and its medicinal preparations by nonaqueous capillary electrophoresis[J]. J Sep Sci, 2004, 27(7 - 8): 569-575.

[9] Zhou L, Zuo Z, Chow MSS. Danshen: an overview of its chemistry, pharmacology, pharmacokinetics, and clinical use[J]. J Clin Pharmacol, 2005, 45(12): 1345-1359.

[10] Sun J, Tan BK, Huang SH, et al. Effects of natural products on ischemic heart diseases and cardiovascular system[J]. Acta Pharmacol Sin, 2002, 23(12): 1142-1151.

[11] Fish JM, Welchons DR, Kim YS, et al. Dimethyl lithospermate B, an extract of Danshen, suppresses arrhythmogenesis associated with the Brugada syndrome[J]. Circulation, 2006, 113(11): 1393-1400.

[12] Chang PN, Mao JC, Huang SH, et al. Analysis of cardioprotective effects using purified *Salvia miltiorrhiza* extract on isolated rat hearts[J]. J Pharmacol Sci, 2006, 101(3): 245-249.

[13] Jang SI, Kim HJ, Kim YJ, et al. Tanshinone IIA inhibits LPS-induced NF-kappaB activation in RAW 264.7 cells: Possible involvement of the NIK IKK, ERK1/2, p38 and JNK pathways[J]. Eur JPharmacol, 2006, 542(1-3): 1-7.

[14] Li W, Li J, Ashok M, et al. A cardiovascular drug rescues mice from lethal sepsis by selectively attenuating a late-acting proinflammatory mediator, high mobility group box 1[J]. J Immunol, 2007, 178(6): 3856-3864.

[15] Lin R, Wang WR, Liu JT, et al. Protective effect of tanshinone IIA on human umbilical vein endothelial cell injured by hydrogen peroxide and its mechanism[J]. J Ethnopharmacol, 2006, 108(2): 217-222.

[16] Wang AM, Sha SH, Lesniak W, et al. Tanshinone (Salviae miltiorrhizae extract) preparations attenuate aminoglycoside-induced free radical formation in vitro and ototoxicity *in vivo*[J]. Antimicrob Agents Chemother, 2003, 47(6): 1836-1841.

[17] Fu L, Han B, Zhou Y, et al. The anticancer properties of tanshinones and the pharmacological effects of their active

ingredients[J]. Front Pharmacol, 2020, 11: 193.
[18] 卓怡呈, 刘程豪, 张示杰. 一种多房棘球蚴原头节提取筛选方法[P]. CN114606176A, 2022-06-10.
[19] Hemer S, Brehm K. *In vitro* efficacy of the anticancer drug imatinib on *Echinococcus multilocularis* larvae [J]. Int JAntimicrob Agents, 2012, 40(5): 458-462.
[20] Zhou L, Sui H, Wang T, et al. Tanshinone IIAreduces secretion of proangiogenic factors and inhibitsangiogenesis in human colorectal cancer[J]. OncolRep, 2020, 43(4): 1159-1168.
[21] Zhou LH, Hu Q, Sui H, et al. Tanshinone II--a inhibits angiogenesis through down regulation of COX-2 in human colorectal cancer[J]. Asian Pac J Cancer Prev, 2012, 13(9): 4453-4458.
[22] Bai Y, Zhang L, Fang X, et al. Tanshinone IIA enhances chemosensitivity of colon cancer cells by suppressing nuclear factor-κB[J]. Exp TherMed, 2016, 11(3): 1085-1089.
[23] Jung JH, Kwon TR, Jeong SJ, et al. Apoptosis induced by tanshinone IIA and cryptotanshinone is mediated by distinct JAK/STAT3/5 and SHP1/2 signaling in chronic myeloid leukemia K562 cells[J]. EvidBased Complement Alternat Med, 2013, 2013.
[24] 谭小武, 姜慧娇, 俞晓凡, 等. 黄腐酚对体外多房棘球蚴原头节活性的影响[J]. 中国病原生物学杂志, 2021, 16(2): 131-136.
[25] 裴彩霞, 汪晓敏, 吴永灿, 等. 桔梗皂苷D通过Bax/Bcl-2/Caspase-3信号通路抑制细胞凋亡保护急性肺损伤的机制研究[J]. 世界科学技术-中医药现代化, 2021, 23(10): 3551-3558.
[26] Tait SWG, Oberst A, Quarato G, et al. Widespread mitochondrial depletion via mitophagy does not compromise necroptosis[J]. Cell Rep, 2013, 5(4): 878-885.
[27] Banjara S, Suraweera CD, Hinds MG, et al. The Bcl-2 family: ancient origins, conserved structures, and divergent mechanisms [J]. Biomolecules, 2020, 10(1): 128.
[28] Yao S, Tian C, Ding Y, et al. Down-regulation of Kr ppel-like factor-4 by microRNA-135a-5p promotes proliferation and metastasis in hepatocellular carcinoma by transforming growth factor-β1[J]. Oncotarget, 2016, 7(27): 42566.
[29] Li FL, Xu R, Zeng Q, et al. Tanshinone IIA inhibits growth of keratinocytes through cell cycle arrest and apoptosis: underlying treatment mechanism of psoriasis[J]. Evid Based Complement Alternat Med, 2012, 2012.
[30] Anzenbacher P, Anzenbacherova E. Cytochromes P450 and metabolism of xenobiotics[J]. Cell Mol Life Sci, 2001, 58(5): 737-747.
[31] Zeeshan HMA, Lee GH, Kim HR, et al. Endoplasmic reticulum stress and associated ROS[J]. Int J Mol Sci, 2016, 17(3): 327.
[32] Chiu TL, Su CC. Tanshinone IIA induces apoptosis in human lung cancer A549 cells through the induction of reactive oxygen species and decreasing the mitochondrial membrane potential [J]. Int J Mol Med, 2010, 25(2): 231-236.
[33] Koziol U, Rauschendorfer T, Zanon Rodr guez L, et al. The unique stem cell system of the immortal larva of the human parasite Echinococcus multilocularis[J]. Evodevo, 2014, 5(1): 1-23.
[34] Kuster T, Hermann C, Hemphill A, et al. Subcutaneous infection model facilitates treatment assessment of secondary Alveolar echinococcosis in mice[J]. PLoS Negl Trop Dis, 2013, 7(5): e2235.
[35] 刘锡娟, 丁慧荣, 张宏. 用DAPI和Hoechst33342染色法测定DNA的流式细胞方法探讨[J]. 北京大学学报(医学版), 2010, 42(4): 480-484.
[36] Cheng Z, Xu Z, Tian H, et al. In vitro and in vivo efficacies of the EGFR/MEK/ERK signaling inhibitors in the treatment of Alveolar Echinococcosis [J]. Antimicrob Agents Chemother, 2020, 64(8): e00341-20.
[37] Xue J, Jin X, Wan X, et al. Effects and mechanism of tanshinone II A in proliferation, apoptosis, and migration of human colon cancer cells[J]. Med Sci Monit, 2019(25): 4793.

【收稿日期】 2022-12-25 【修回日期】 2023-03-11

(上接688页)

[18] Sun P, Nie K, Zhu Y, et al. A mosquito salivary protein promotes flavivirus transmission by activation of autophagy [J]. Nat Commun, 2020, 11(1): 260.
[19] Mukherjee D, Das S, Begum F, et al. The mosquito immune system and the life of dengue virus: What we know and do not know[J]. Pathogens, 2019, 8(2): 77.
[20] Xiao X, Liu Y, Zhang X, et al. Complement-related proteins control the flavivirus infection of *Aedes aegypti* by inducing antimicrobial peptides[J]. PLoS Pathog, 2014, 10(4): e1004027.
[21] Schroeder S, Pott F, Niemeyer D, et al. Interferon antagonism by SARS-CoV-2: a functional study using reverse genetics [J]. Lancet Microbe, 2021, 2(5): e210-e218.
[22] Michalska A, Blaszczyk K, Wesoly J, et al. A positive feedback amplifier circuit that regulates interferon (IFN)-stimulated gene expression and controls type I and type II IFN responses[J]. Front Immunol, 2018(9): 1135.
[23] Bogunovic D, Byun M, Durfee LA, et al. Mycobacterial disease and impaired IFN-γ immunity in humans with inherited ISG15 deficiency[J]. Science, 2012, 337(6102): 1684-1688.
[24] Andrejeva J, Norsted H, Habjan M, et al. ISG56/IFIT1 is primarily responsible for interferon-induced changes to patterns of parainfluenza virus type 5 transcription and protein synthesis [J]. J Gen Virol, 2013, 94(Pt 1): 59-68.
[25] Valenzuela-Leon PC, Shrivastava G, Martin-Martin I, et al. Multiple salivary proteins from *Aedes aegypti* mosquito bind to the Zika virus envelope protein[J]. Viruses, 2022, 14(2): 221.
[26] Marsh M, Helenius A. Virus entry: open sesame[J]. Cell, 2006, 124(4): 729-740.

【收稿日期】 2022-12-15 【修回日期】 2023-03-05